Sensors and Actuators B 216 (2015) 629–637

Contents lists available at ScienceDirect

Sensors and Actuators B: Chemical

journal homepage: www.elsevier.com/locate/snb

Functionalization of bamboo-like carbon nanotubes with 3-mercaptophenylboronic acid-modified gold nanoparticles for the development of a hybrid glucose enzyme electrochemical biosensor

Marcos Eguílaz [a], Reynaldo Villalonga [b], J.M. Pingarrón [b], Nancy F. Ferreyra [a,*], Gustavo A. Rivas [a,*]

[a] INFIQC, Dpto. de Fisicoquímica, Facultad de Ciencias Químicas, Universidad Nacional de Córdoba, 5000 Córdoba, Argentina
[b] Dpto de Química Analítica, Facultad de Ciencias Químicas, Universidad Complutense de Madrid, 28040 Madrid, Spain

ARTICLE INFO

Article history:
Received 21 January 2015
Received in revised form 25 March 2015
Accepted 30 March 2015
Available online 20 April 2015

Keywords:
Bamboo-like multiwalled carbon nanotubes
Carbon nanotubes dispersion
Polyethylenimine
Glucose oxidase
Boronic acid
Gold nanoparticles
Amperometric glucose biosensor

ABSTRACT

We report for the first time a sensitive and selective glucose biosensor based on the immobilization at glassy carbon electrodes (GCE) of a new hybrid nanomaterial consisting of gold nanoparticles functionalized with 3-mercaptophenyl boronic acid (AuNPs-B(OH)$_2$) and bamboo-like multiwall carbon nanotubes (bMWCNT) dispersed in hyperbranched polyethyleneimine (PEI). The presence of boronic acid residues allowed the supramolecular immobilization of glucose oxidase (GOx) as a model glycoenzyme while the hybrid nanomaterial Au(NP)-bMWCNT produces a synergistic effect on the catalytic detection of the enzymatically generated hydrogen peroxide. The resulting functionalized nanomaterials were characterized by TEM, FT-IR and electrochemical techniques. The sensitivity at 0.700 V was (3.26 ± 0.03) mA M^{-1} (28.6 mA M^{-1} cm^{-2}), with a linear range between 2.50×10^{-4} M and 5.00×10^{-3} M, a detection limit of 0.8 μM and a quantification limit of 2.4 μM. The biocatalytic layer demonstrated to be highly reproducible with R.S.D. values of 8.6% for 10 successive amperometric calibrations using the same surface, and 4.5% for ten different bioelectrodes. The sensitivity of the biosensor after 14 days of storage at 4 °C remained at 86.1% of its original value. The combination of the excellent dispersing properties of PEI, the stability of the bMWCNT-PEI dispersion, the synergistic effect of AuNPs-B(OH)$_2$ and bMWCNT towards the electrooxidation of hydrogen peroxide, and the robust immobilization of GOx at AuNP-B(OH)$_2$ allowed building a sensitive, reproducible and stable amperometric biosensor for the quantification of glucose in beverages and milk samples.

1. Introduction

The design of novel bioanalytical platforms able to conjugate an efficient immobilization of biomolecules with an improved electroanalytical performance is a real challenge in the field of electrochemical biosensors [1]. In this context, electroconductive nanosized materials have been extensively used in the last decade due to their unique properties such as high surface-to-volume ratio, biocompatibility, capability of connection to the active sites of the biomolecules and relatively easy functionalization [2,3].

Carbon nanotubes (CNTs) and nanoparticles (NPs) of metals and metal oxides have played an important role due to their excellent electronic and structural properties [3–6]. Current investigations are focused on the development of innovative functionalization methods using novel hybrid materials and modified ligands to obtain sensing surfaces that combine the best properties of each material [7]. The use of nanohybrids involving CNTs and NPs for the preparation of electrochemical biosensors has attracted great attention in the last few years [8–13]. This combination allowed developing biosensors with improved biocompatibility, stability and sensitivity compared to those obtained using NPs and CNTs separately.

One of the most used alternatives for the preparation of CNTs derivatives is based on the non-covalent modification with polymers, surfactants or aromatic molecules [14–17]. In all cases the wrapping effect of these molecules produces a modification of their potential energy that avoids the aggregation of CNTs and allows stable CNTs dispersions in polar solvents [18]. The great advantage of this wrapping effect is that the electronic structure of CNTs

* Corresponding authors. Tel.: +54 351 5353866; fax: +54 351 4334188.
E-mail addresses: ferreyra@fcq.unc.edu.ar (N.F. Ferreyra), grivas@fcq.unc.edu.ar, rivasgus@yahoo.com.ar (G.A. Rivas).

http://dx.doi.org/10.1016/j.snb.2015.03.112
0925-4005/

is preserved [19]. Depending on the charge of the polymer, it is possible to assemble poly-electrolytes of opposite charge such as enzymes [20], DNA [21] or nanoparticles to prepare supramolecular architectures suitable for different electroanalytical applications [17].

The possibility of tailor-made design of nanomaterials with specific properties by manipulation of the capping ligands or modified molecules represents a very promising alternative for the immobilization of biomolecules. In this sense, the use of boronic acid derivatives has been proposed as an interesting strategy due to the selective formation of cyclic boronate esters between the cis-diol groups of carbohydrates and the boronic acid groups [22]. This interaction has been employed for the detection of carbohydrates [23], bacteria [24] and glycoproteins such as glycated hemoglobin [25,26], hemagglutinin [27] and α-fetoprotein [28] as well as for the oriented immobilization of antibodies in the construction of immunosensors [29,30]. Boronic acid functionalized-gold nanoparticles (AuNPs) have been successfully used for the detection of carbohydrates [31], antibiotics [32], and for signal amplification [33–35]. The selective and supramolecular immobilization of the glycoprotein horseradish peroxidase (HRP) has been also reported for the construction of a reagentless enzyme electrochemical biosensor by electropolymerization of AuNPs polyfunctionalized with p-aminothiophenol, 2-mercaptoethanesulfonic acid and 3-mercaptophenyl boronic [36].

In this work, we combined gold nanoparticles functionalized with 3-mercaptophenyl boronic acid (AuNPs-B$(OH)_2$) with a dispersion of bamboo-like multiwall carbon nanotubes (bMWCNT) in hyperbranched polyethyleneimine (PEI). The aim of this work was to design a novel hybrid nanomaterial integrating the inherent advantages of both components. The presence of boronic acid residues allows the supramolecular immobilization of glycoenzymes, while bMWCNT-PEI dispersion offers an optimal platform for the transduction of the electrochemical response. To the best of our knowledge, this is the first report using this combination of polyfunctionalized nanomaterials. To evaluate the capabilities of this new electrochemical biointerface, we selected the glycoprotein glucose oxidase (GOx) as a model enzyme to develop a glucose biosensor and we evaluated the analytical performance from the oxidation of the enzymatically generated hydrogen peroxide. The bioelectrode was also used to quantify glucose in real samples.

2. Experimental

2.1. Chemicals and solutions

β-D-(+)-glucose (Glu) was obtained from Merck. Hydrogen peroxide (30%, v/v aqueous solution), NaH_2PO_4 and Na_2HPO_4 were purchased from Baker. Glucose oxidase (GOx) (Type X-S, Aspergillus niger, EC 1.1.3.4, 157,500 units/g of solid), hyperbranched polyethyleneimine (PEI, 50%, w/v, average MW 750,000), citrate stabilized gold colloid (AuNPs-cit, 20 nm diameter), $HAuCl_4$, $NaBH_4$, mercaptopropionic acid (MPA) and 3-mercaptophenyl boronic acid (MPhBA), were obtained from Sigma. Bamboo-type multiwalled carbon nanotubes powder ((30 ± 10) nm diameter, length 1–5 μm and 98.92% purity) was obtained from NanoLab (U.S.A.) and used pristine without chemical purification or activation. All other chemicals were of analytical grade and were used without further purification. Commercial soft drinks (Pepsi®, Gatorade® and Red Bull®) and baby milk samples ("Crecer 1" milk for babies from 0 to 6 months, Argentine dairy company "La Serenísima") were acquired from a local market.

PEI solutions were prepared in water. The stock solutions of GOx, Glu, and H_2O_2 were prepared in a 0.050 M phosphate buffer solution pH 7.40. The same buffer solution was employed as supporting electrolyte. Ultrapure water (ρ = 18.2 MΩ cm) from a Millipore-MilliQ system was used for preparing all aqueous solutions.

2.2. Apparatus

Sonication treatments were carried out with an ultrasonic processor VCX 130W (Sonics and Materials, Inc.) of 20 kHz frequency with a titanium alloy microtip of 3 mm diameter. An Allegra™ 21 ultracentrifuge (Beckman Coulter) with a F2402H rotor was used to centrifuge the samples after sonication.

Electrochemical experiments were carried out with a CHI Model 600D and TEQ_04 potentiostats using a three-electrodes glass electrochemical cell. Glassy carbon electrodes (GCE, CH Instruments, 3 mm diameter) modified with bMWCNTs-PEI and functionalized with the gold nanoparticles were used as working electrodes. A platinum wire and a Ag/AgCl, 3 M NaCl (BAS, Model RE-5B) were used as auxiliary and reference electrodes, respectively. All potentials are referred to this reference electrode. A magnetic stirrer under controlled speed provided the convective transport during the amperometric measurements.

FT-IR spectra were acquired with a PerkinElmer instrument. UV–vis absorption spectra were obtained with a Shimadzu UV-1700 Pharma spectrophotometer using a quartz cuvette of 1 mm path length. Proper dilution of samples was performed before obtaining the UV–vis spectra. Transmission electron microscopy (TEM) images were obtained using a JEM-2000 FX JEOL microscope. The samples were obtained by dropping the dispersion of the nanomaterial onto the TEM grids and drying in air at room temperature.

2.3. Preparation of the nanomaterials

To prepare the polyfunctionalized gold nanoparticles, 66.0 mg of $HAuCl_4$ (168 μmol) were dissolved in 15.0 mL of deaerated dimethyl sulfoxide (DMSO). This solution was added dropwise to 15.0 mL of deaerated DMSO containing 100.0 mg of sodium borohydride, 7.0 μL of MPA (80 μmol) and 6.2 mg of MPhBA (40 μmol) under vigorous stirring. The reaction mixture turned deep brown immediately, although the reaction was allowed to continue for 24 h at room temperature. The functionalized AuNPs were precipitated by adding 30.0 mL of CH_3CN, collected by centrifugation, and washed with 60.0 mL of CH_3CN:DMSO (1:1 v/v), 60.0 mL of ethanol and 20.0 mL of diethyl ether. The AuNPs functionalized with MPA and MPhBA, named as AuNPs-B$(OH)_2$, were isolated by centrifugation and dried under N_2.

The dispersion of bMWCNTs in PEI was obtained by mixing 1.0 mg of bMWCNTs with 1.0 mL of a PEI solution (4.0 mg mL^{-1} in water) followed by sonication with a sonicator probe for 5.0 min. The amplitude was 50% and the sample was kept in an ice-bath during the procedure. After this treatment, the samples were centrifuged at 9000 rpm for 15 min and the supernatant was collected.

2.4. Preparation of the nanohybrid surfaces

2.4.1. GCE/bMWCNTs-PEI/AuNPs-B$(OH)_2$/GOx

GCE surfaces were polished with alumina slurries of 1.0, 0.3 and 0.05 μm for 1 min each, rinsed thoroughly with deionized water and sonicated for 30 s in water. The electrode was carefully dried under a N_2 stream. GCE/bMWCNTs-PEI was prepared by casting 10 μL of the dispersion onto the GCE surface and the solvent was evaporated at room temperature for 60 min.

AuNPs-B$(OH)_2$ were adsorbed at GCE/bMWCNTs-PEI electrode for 30 min from a 20 μL aliquot of a 3.0 mg mL^{-1} AuNPs-B$(OH)_2$ solution prepared in water deposited onto the electrode avoiding solvent evaporation. The modified electrode, named GCE/bMWCNTs-PEI/AuNPs-B$(OH)_2$, was exhaustively rinsed with

0.050 M phosphate buffer solution pH 7.40 to remove the weakly adsorbed nanoparticles.

GOx was immobilized at GCE/bMWCNTs-PEI/AuNPs-B(OH)$_2$ for 15 min from an aliquot of 20 μL of a 3.0 mg mL^{-1} enzyme solution prepared in 0.050 M phosphate buffer pH 7.40 and avoiding the solvent evaporation. The bioelectrode, named as GCE/bMWCNTs-PEI/AuNPs-B(OH)$_2$/GOx, was rinsed several times with 0.050 M phosphate buffer solution pH 7.40 and stored at 4 °C.

For comparison, other electrodes were also prepared:

GCE/PEI: by dropping 10 μL of 4.0 mg mL^{-1} PEI solution previously sonicated and centrifuged using the same experimental conditions as those for preparing bMWCNT-PEI dispersion (Section 2.3).

GCE/PEI-AuNP-B(OH)$_2$: same conditions as GCE/PEI followed by the deposition of 20 μL of 3.0 mg mL^{-1} AuNP-B(OH)$_2$.

GCE/bMWCNT-PEI: by dropping 10 μL of bMWCNT-PEI dispersion sonicated and centrifuged using the conditions previously described (Section 2.3).

2.4.2. Quartz/CHIT/AuNPs-B(OH)$_2$/GOx

The quartz surface was treated by sonication for 20 min in an ethanolic solution of 1.0% (w/v) NaOH. After exhaustive rinsing with water, 1.0 mg mL^{-1} PEI was adsorbed for 1 h, followed by the adsorption of 0.6 mg mL^{-1} AuNPs-B(OH)$_2$ for 1 h. Finally, GOx was allowed to interact for increasing incubation time using a 3.0 mg mL^{-1} GOx solution. Equivalent conditions were used for the experiments performed using AuNPs-citrate.

After each adsorption step, the solution was removed and the cuvette was repeatedly rinsed with deionized water. UV–vis spectral curves were obtained in water to avoid drying of the surface.

2.5. Procedure

Cyclic voltammetry (CV) was carried out in the potential range between −0.200 V and 0.800 V at a scan rate of 0.100 V s^{-1}. Amperometric experiments were performed in stirred solutions by applying a working potential of 0.700 V and allowing the transient current to reach a steady-state value prior to the addition of the analyte and the subsequent current monitoring. All experiments were conducted at room temperature in a 0.050 M phosphate buffer solution pH 7.40.

The electroactive area of the different electrodes was obtained by CV using a 5.0×10^{-4} M ferrocene methanol (FcMeOH) solution as redox probe. The areas were calculated using the Randles equation considering a diffusion coefficient of FcMeOH of 7.6×10^{-6} cm^2 s^{-1} [37].

2.6. Determination of glucose in real samples

Deproteinized milk and commercial soft drinks samples were used to evaluate the analytical performance of the proposed biosensor. To obtain deproteinized milk, 100 μL of 12.2 M HCl solution was added to 1.0 mL of milk and shaken for 60 s. After centrifugation at 12,000 rpm for 15 min, the supernatant was collected and the pH was neutralized to 7.0 by addition of 1 M NaOH. A 50 μL aliquot of deproteinized milk was transferred to the electrochemical cell containing 5.0 mL of 0.050 M phosphate buffer solution pH 7.40. Aliquots of 10 μL of Pepsi® and Gatorade® samples or 10 μL of 1:1 Red Bull® stock solution (diluted with the phosphate buffer) were transferred to the electrochemical cell containing 5.0 mL of 0.050 M phosphate buffer solution pH 7.40. In all cases, the determination of glucose was performed by amperometry at 0.700 V and the glucose content was determined by using the standard additions method.

3. Results and discussion

Scheme 1 shows the synthesis of AuNPs and the steps involved in the preparation of the supramolecular architecture obtained by the immobilization of GOx at the GCE modified with the nanohybrid bMWCNT-PEI/AuNP-B(OH)$_2$.

3.1. Preparation and characterization of polyfunctionalized gold nanoparticles

Polyfunctionalized gold NPs were synthesized by fast reduction of $AuCl_4^-$ with $NaBH_4$ in a DMSO solution containing MPhBA and MPA as indicated in Scheme 1. The presence of the thiolated ligands in the reaction medium ensures the fast coating of the growing gold colloids [38]. The thiol-derivatives used as capping ligands were selected to give some particular properties to the AuNPs. MPhBA acts as recognition element for GOx immobilization by reacting with the vicinal diols of the glycoenzyme, while MPA favors the solubility and stability of the resulting AuNPs. A MPhBA/MPA molar ratio 1:2 was selected to get the best compromise between solubility, stability and recognition ability.

The polyfunctionalized AuNPs were characterized by FTIR, UV–vis and TEM. UV–vis absorption spectrum exhibits an absorbance peak at 530 nm due to the dark red and water-soluble nanoparticles (Fig. 1A). Fig. 1B shows the FT-IR spectrum of the polyfunctionalized AuNPs named AuNPs-B(OH)$_2$. A very strong and broad band appears in the range from 3800 to 2600 cm^{-1}, which can be attributed to the overlapped O–H stretching vibrations corresponding to the hydroxyl groups of MPhBA and MPA. In addition, the presence of the MPA residues can be supported by the stretching vibration band of the C=O bond at 1662 cm^{-1}. Regarding the presence of boronic acid residues, it is confirmed by the characteristics B–O stretching vibration band at 1344 cm^{-1} and the strong band at 1002 cm^{-1} attributed to the B–O–H deformation [39]. These signals confirmed the presence of the capping ligands on the surface of the polyfunctionalized AuNPs. According to the TEM image of the synthesized AuNPs (Fig. 1C) and their size distribution obtained from several TEM images (Fig. 1D), the nanoparticles are rather polydispersed although the particle size are mostly located in a range from 3.7 to 7.2 nm.

3.2. Preparation of the hybrid nanomaterial [bMWCNT-PEI/AuNPs-B(OH)$_2$]

PEI has demonstrated to be an efficient dispersing agent for MWCNTs [40,41]. The adequate combination of ultracavitation and centrifugation was essential to obtain successful dispersions of bMWCNTs preserving their unique electrocatalytic properties due to the presence of the defects regularly located along the walls [41]. According to these results, the CNT dispersion was prepared by sonication of 1.0 mg mL^{-1} bMWCNTs with 4.0 mg mL^{-1} PEI in water for 300 s followed by centrifugation at 9000 rpm for 15 min. To prepare the composite material, GCE was modified by drop-coating with 10 μL of bMWCNTs-PEI on the electrode surface. The positively charged amine groups of PEI were used for the electrostatic adsorption of AuNPs-B(OH)$_2$, negatively charged at the working pH. Fig. 2 shows a TEM image of the hybrid material bMWCNTs-PEI/AuNPs-B(OH)$_2$, where is possible to observe the attachment of polyfunctionalized AuNPs to the PEI-wrapped-bMWCNTs surface.

Considering that the electrode will be used as a platform for developing a glucose biosensor and that the analytical signal will be obtained from the oxidation of the hydrogen peroxide generated during the regeneration of GOx in the presence of the natural mediator, oxygen, we evaluated the electrochemical response of different electrodes to hydrogen peroxide. Fig. 3A shows cyclic voltammograms of 1.0×10^{-2} M H_2O_2 obtained at

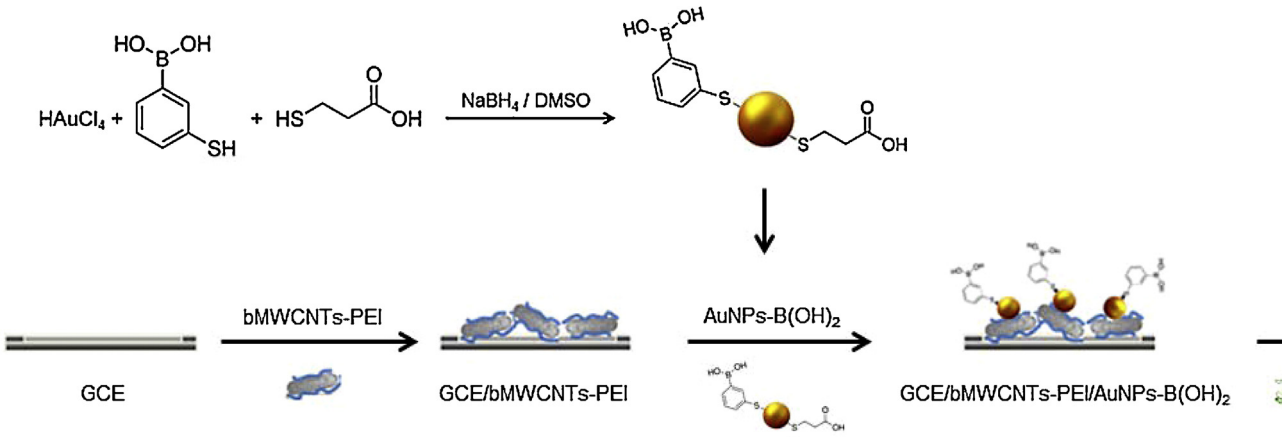

Scheme 1. Schematic display of the steps involved in the preparation of the GCE/bMWCNTs-PEI/AuNPs-B(OH)$_2$/GOx biosensor.

GCE/PEI (a), GCE/PEI/AuNPs-B(OH)$_2$ (b), GCE/bMWCNTs-PEI (c) and GCE/bMWCNTs-PEI/AuNPs-B(OH)$_2$ (d). Compared to GCE/PEI, at GCE/PEI/AuNPs-B(OH)$_2$ there is a decrease in the overvoltage for hydrogen peroxide reduction and oxidation and an increase of the oxidation and reduction currents mainly due to the electrocatalytic properties of the polyfunctionalized gold nanoparticles. At GCE/bMWCNTs-PEI, the increase in the electroactive surface and the presence of the edge-like defects along the bamboo shaped carbon nanotubes, are responsible for the larger hydrogen peroxide oxidation and reduction currents compared to GCE/PEI. More interestingly, a remarkable increase in the oxidation current is observed at GCE/bMWCNTs-PEI/AuNPs-B(OH)$_2$, suggesting a synergistic effect between bMWCNT-PEI and AuNPs-B(OH)$_2$.

The effect of the adsorption time of 3.0 mg mL^{-1} AuNPs-B(OH)$_2$ (from 0 to 60 min) on the amperometric response of hydrogen peroxide was evaluated at 0.700 V. Fig. 3B displays the sensitivity of GCE/bMWCNT-PEI/AuNPs-B(OH)$_2$, obtained from the slope values of the corresponding calibration plots, as a function of the nanoparticles adsorption time. The sensitivity increases sharply with time up to 15 min and levels off after 30 min, indicating that the surface of the electrode was fully covered under these experimental conditions.

3.3. Effect of boronic acid functionalities on GOx immobilization

The capability of boronic acid to recognize the glycoprotein GOx was evaluated by comparing the electrochemical behavior

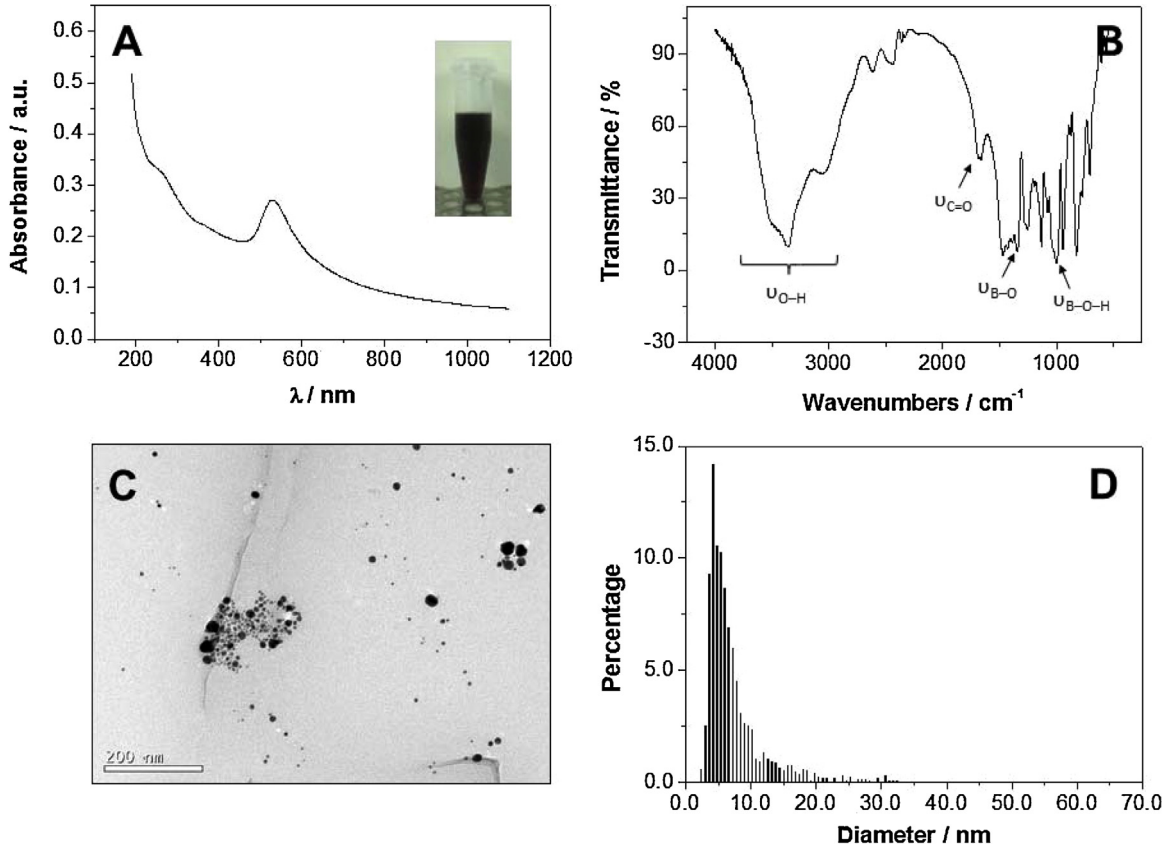

Fig. 1. (A) UV–vis absorption spectra, (B) FT-IR spectra, (C) TEM micrograph and (D) distribution size of the AuNPs-B(OH)$_2$ (n = 1824).

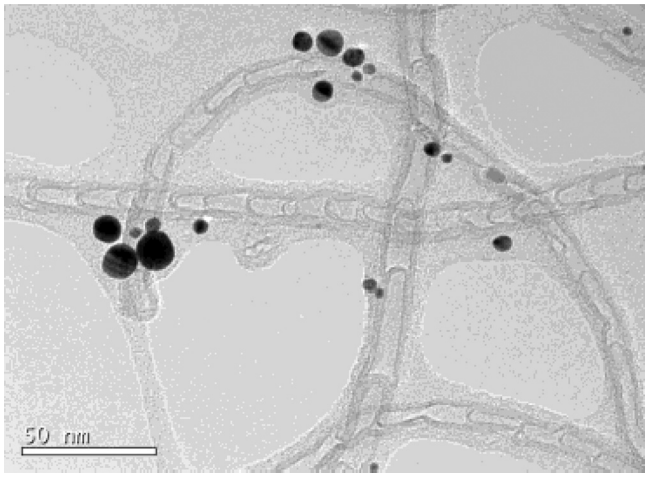

Fig. 2. TEM micrograph of bMWCNTs/AuNPs-B(OH)$_2$. Conditions: bMWCNTs (1.0 mg mL^{-1}) were dispersed in 3.0 mg mL^{-1} prepared in water. Sonication time: 5.0 min, acoustic amplitude: 50% and centrifugation: 9000 rpm for 15 min. The dispersion of the hybrid material bMWCNTs-PEI/AuNPs-B(OH)$_2$ was obtained by preparing a 1:1 (v/v) mixture, comprising a 1.0 mg mL^{-1} AuNPs-B(OH)$_2$ solution prepared in water and the bMWCNTs-PEI dispersion.

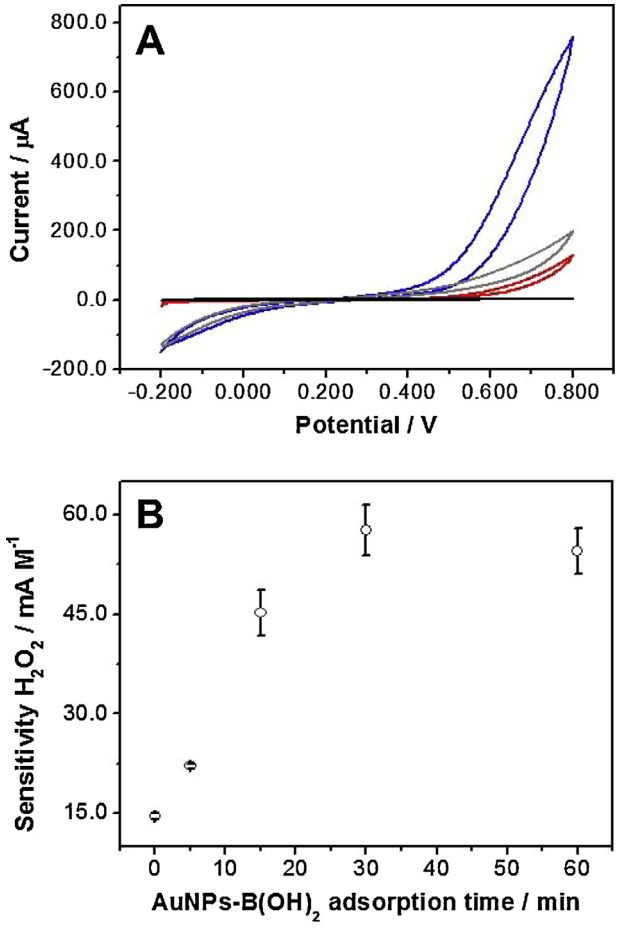

Fig. 3. (A) Cyclic voltammograms of 0.010 M H_2O_2 at $\nu = 0.100$ V s^{-1} obtained at GCE/PEI (a), GCE/PEI/AuNPs-B(OH)$_2$ (b), GCE/bMWCNTs-PEI (c) and GCE/bMWCNTs-PEI/AuNPs-B(OH)$_2$ (d). (B) Sensitivity towards H_2O_2 obtained from amperometric experiments at GCE/bMWCNTs-PEI/AuNPs-B(OH)$_2$ as a function of the adsorption time of 3.0 mg mL^{-1} AuNPs-B(OH)$_2$. Experimental conditions: $E_{app} = 0.700$ V, supporting electrolyte 0.050 M phosphate buffer solution pH 7.40.

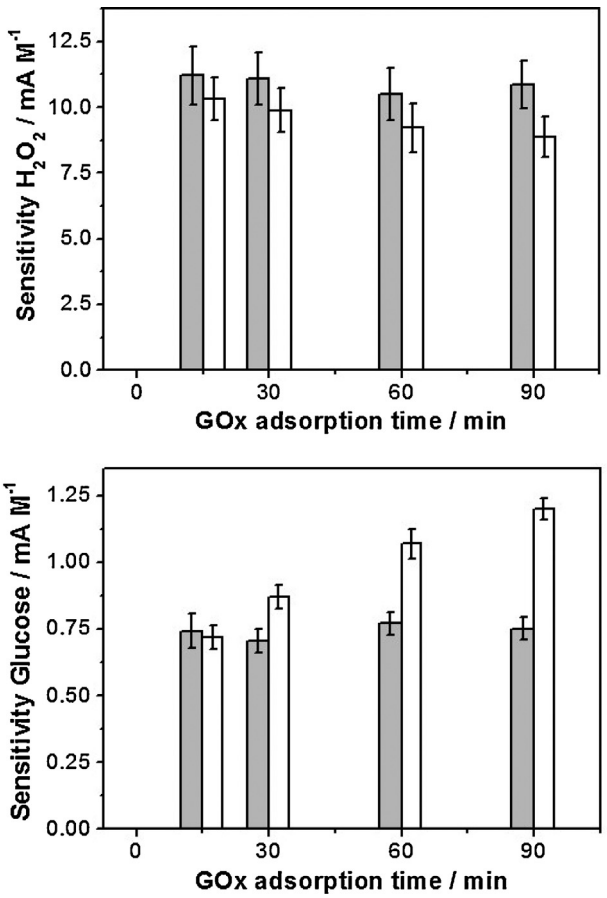

Fig. 4. Sensitivity towards (A) H_2O_2 and (B) glucose obtained from amperometric experiments as a function of GOx interaction time obtained at GCE/bMWCNTs-PEI/AuNPs-citrate (gray) and GCE/bMWCNTs-PEI/AuNPs-B(OH)$_2$/GOx (white). AuNPs-B(OH)$_2$ concentration: 0.6 mg mL^{-1}; AuNPs-B(OH)$_2$ adsorption time: 30 min; GOx concentration: 3.0 mg mL^{-1}. Equivalent conditions were used for the experiments performed using AuNPs-citrate. $E_{app} = 0.700$ V, supporting electrolyte 0.050 M phosphate buffer solution pH 7.40.

of biosensors prepared with equivalent amount of AuNPs-B(OH)$_2$ and citrate stabilized gold nanoparticles (AuNPs-cit). The amount of adsorbed nanoparticles was checked by cyclic voltammetry in 0.50 M sulfuric acid solution by integrating the charge corresponding to the gold oxides reduction peak.

Fig. 4 compares the sensitivity attained for hydrogen peroxide (A) and glucose (B) as a function of GOx interaction time at GCE/bMWCNTs-PEI/AuNPs-B(OH)$_2$/GOx (white bars) and GCE/bMWCNTs-PEI/AuNPs-cit/GOx (gray bars). The sensitivities for hydrogen peroxide, used as control, do not show significant differences neither at GCE/bMWCNTs-PEI/AuNPs-B(OH)$_2$/GOx nor at GCE/bMWCNTs-PEI/AuNPs-cit/GOx (Fig. 4A), since hydrogen peroxide is not substrate of the enzyme. On the contrary, the sensitivity to glucose largely increases with the interaction time of GOx at GCE/bMWCNTs-PEI/AuNPs-B(OH)$_2$/GOx (Fig. 4B), while no significant changes are observed at GCE/bMWCNTs-PEI/AuNPs-cit/GOx (Fig. 4B), demonstrating the specific interaction between the glycoprotein and AuNPs-B(OH)$_2$.

The complex formation between AuNPs-B(OH)$_2$ and GOx was also confirmed by UV–vis spectroscopy (not shown). The adsorption of PEI and AuNPs-B(OH)$_2$ was performed from 1.0 mg mL^{-1} PEI and 0.6 mg mL^{-1} AuNPs-B(OH)$_2$ solutions for 1 h, by filling the quartz cuvette treated with NaOH/ethanol followed by copiously rinsed with water. GOx linking was performed from a 3.0 mg mL^{-1} solution for increasing incubation time. A characteristic absorption peak corresponding to the polypeptides chains was

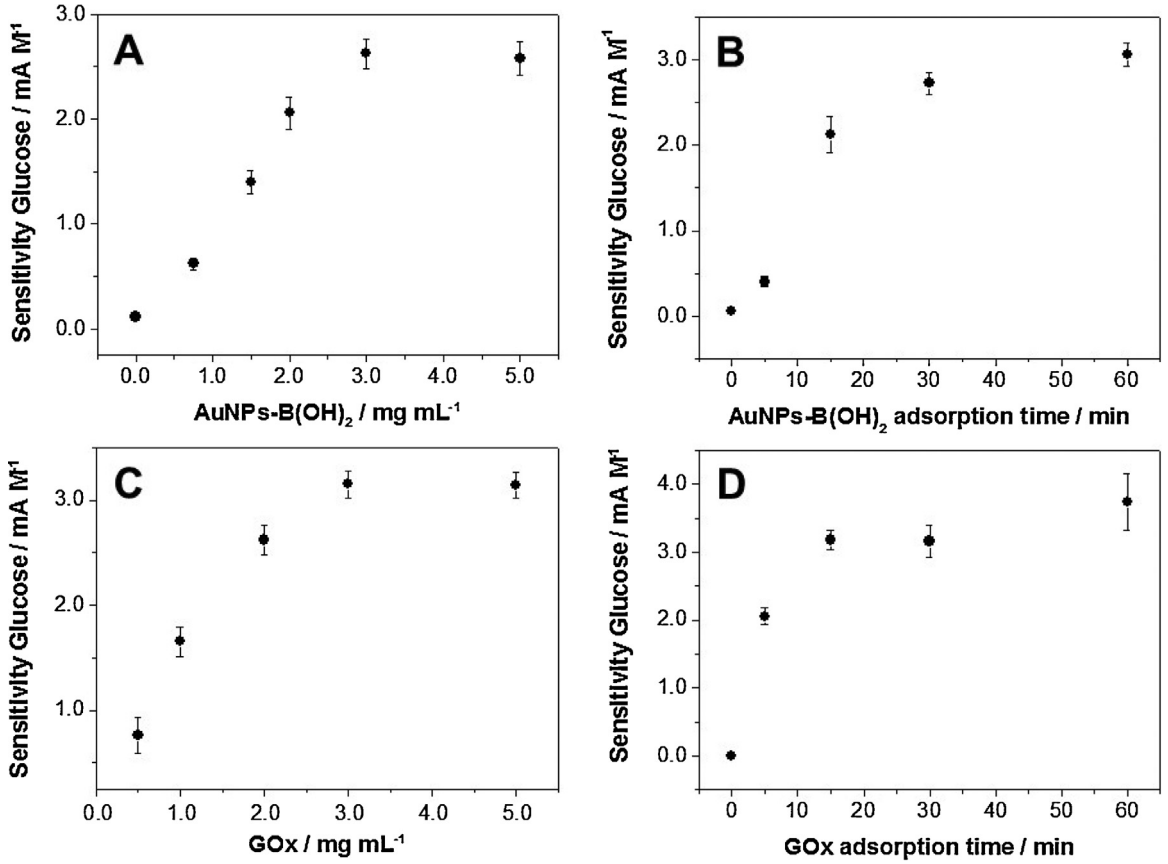

Fig. 5. Sensitivity towards glucose obtained from amperometric experiments at GCE/bMWCNTs-PEI/AuNPs-B(OH)$_2$/GOx biosensor as a function of (A) AuNPs-B(OH)$_2$ concentration (*Conditions*: AuNPs-B(OH)$_2$ adsorption time: 30 min, GOx concentration: 2.0 mg mL^{-1}, GOx interaction time: 30 min); (B) AuNPs-B(OH)$_2$ adsorption time (Conditions: AuNPs-B(OH)$_2$ concentration: 3.0 mg mL^{-1}, GOx concentration: 2.0 mg mL^{-1}, GOx adsorption time: 30 min); (C) GOx concentration (Conditions: AuNPs-B(OH)$_2$ concentration: 3.0 mg mL^{-1}, AuNPs-B(OH)$_2$ adsorption time: 30 min, GOx adsorption time: 30 min); and (D) GOx interaction time (Conditions: AuNPs-B(OH)$_2$ concentration: 3.0 mg mL^{-1}, AuNPs-B(OH)$_2$ adsorption time: 30 min, GOx concentration: 3.0 mg mL^{-1}). E_{app} = 0.700 V, supporting electrolyte 0.050 M phosphate buffer solution pH 7.40.

observed at 277 nm after GOx attachment [42]. Fig. SI1 shows the absorbance at 277 nm as a function of GOx incubation time at Quartz/PEI/AuNPs-B(OH)$_2$ surface (white). The absorbance exhibited a gradual increase with the incubation time of the enzyme in the whole range of reaction times. For comparison, equivalent experiments were performed using AuNPs-citrate (gray). In this case, a slight increase in the absorbance was observed after 15 and 30 min of enzyme incubation, but no changes were observed for longer incubation times, clearly demonstrating the capability of AuNPs-B(OH)$_2$ to immobilize GOx compared to AuNPs-citrate.

3.4. Optimization of the [GCE/bMWCNTs-PEI/AuNPs-B(OH)$_2$/GOx] biosensor

The synergistic effect of bMWCNTs-PEI/AuNPs-B(OH)$_2$ towards the electrocatalytic oxidation of H_2O_2 combined with the ability of the boronic functionalized AuNPs for the recognition of glycoenzymes, allowed the construction of a glucose oxidase based electrochemical biosensor.

The preparation of the enzymatic electrode was optimized by determining the influence of the experimental variables that affect the biosensor response: concentration and adsorption time of AuNPs-B(OH)$_2$ (Fig. 5A and B) and concentration and reaction time of GOx (Fig. 5C and D). Fig. 5A shows the influence of the AuNPs-B(OH)$_2$ concentration on the glucose sensitivity obtained from amperometric experiments performed at 0.700 V at GCE/bMWCNTs-PEI/AuNPs-B(OH)$_2$/GOx. There is a fast increase in sensitivity with AuNPs concentration up to 3.0 mg mL^{-1}. These results could be ascribed to the catalytic properties of AuNP and the larger boronic groups loading on the electrode surface accessible for enzyme immobilization. In order to get the highest glucose sensitivity, 3.0 mg mL^{-1} AuNPs-B(OH)$_2$ was selected for further work. The influence of the adsorption time of AuNPs-B(OH)$_2$ on the glucose sensitivity was also evaluated (Fig. 5B). A sharp increase is observed up to 15 min, with moderate changes for longer incubation times. Accordingly, an incubation time of 30 min was selected as a compromise between the highest sensitivity and adequate preparation time. Moreover, the sensitivity of the biosensor increased progressively with the concentration and reaction time of the enzyme, reaching the highest values after 15 min of GOx interaction from a 3.0 mg mL^{-1} of enzyme solution (Fig. 5C and D).

Under the optimal conditions, the surface coverage of the bioactive GOx (Γ_{GOx}) at the hybrid nanomaterial GCE/bMWCNTs-PEI/AuNPs-B(OH)$_2$, which is the fraction of the enzyme available for the charge transfer, was evaluated using 5.0×10^{-4} M FcMeOH as redox regenerator in N_2-satured 0.100 M phosphate buffer solution pH 7.40 according to the Bourdillon method [43] (see SI).

Γ_{GOx}, was calculated from the biosensor response using the following equation

$$i_{cat} = \frac{nFAk_3\Gamma^*_{GOx}[FcMO^{\bullet+}]}{1 + k_3[FcMO^{\bullet+}]((1/k_2) + (1/k_{red}[Glu]))}$$

where [FcMO$^{\bullet+}$] and [Glu] are the concentrations of the oxidized mediator and substrate, respectively, $k_{red} = k_1k_2/(k_{-1} + k_2)$, and i_{cat} is the catalytic current determined at GCE/bMWCNTs-PEI/AuNPs-B(OH)$_2$/GOx as the difference between the current obtained in the

Table 1
Comparison of the analytical characteristics obtained for GCE/bMWCNTs-PEI/AuNPs-B(OH)$_2$/GOx biosensor with those reported for other glucose biosensors based on hybrid materials of carbon nanotubes and nanoparticles.

Biosensor	Sensitivity	Linear range (M)	LOD (μM)	Stability (%)	Ref.
GCE/MWCNTs-Chit/GOx/ZnONPs/GOx	3.02 mA M^{-1}	6.67×10^{-6} to 1.29×10^{-3}	2.22	93.4 over 10 days	Hu et al. [45]
GCE/MWCNTs-IL-AuNPs/GOx	15.6 mA M^{-1} cm^{-2}	2.0×10^{-3} to 12.0×10^{-3}	–	–	Jia et al. [46]
GCE/MWCNTs-PSS-IL-AuNPs/GOx	–	0 to 20.0×10^{-3}	25	89.7 over 7 days	Li et al. [47]
GCE/MWCNTs-Chit-PtNPs/Con A/GOx	–	1.2×10^{-6} to 2.0×10^{-3}	0.4	94.4 over 10 days	Li et al. [48]
PE(MWCNT-AuNPs-GOx)	2.6 mA M^{-1}	5.0×10^{-5} to 1.0×10^{-3}	17	90 over 8 days	Manso et al. [49]
GCE/MWCNTs-AuNPs/Nf/GOx	0.4 mA M^{-1}	5.0×10^{-5} to 2.2×10^{-2}	20	–	Rakhi et al. [50]
ITO/MWCNTs-IL-Chit/AuNPs/GOx	4.1 mA M^{-1}	1.0×10^{-3} to 10.0×10^{-3}	–	90 over 20 days	Ragutaphy et al. [51]
GCE/MWCNTs-ACS/PtNPs/GOx	113.13 mA M^{-1} cm^{-2}	5.0×10^{-5} to 10.5×10^{-3}	6.18	85 over 8 days	Tsai and Tsai [52]
GCE/MWCNTs-sulfonated-PtNPs/GOx	0.56 mA M^{-1}	1.0×10^{-5} to 6.4×10^{-3}	–	85 over 1 hour	Wang et al. [53]
GCE/(AuNP-Chit/MWCNT)$_8$/GOx	–	6.0×10^{-6} to 5.0×10^{-3}	3	81.3 over 10 days	Wang et al. [54]
GCE/MWCNTs-pDA-AgNPs/GOx/Nf	3.1 mA M^{-1}	5.0×10^{-5} to 1.1×10^{-3}	17	92 over 14 days	Wang et al. [55]
GCE/MWCNTs-PtNPs-GOx-Nf	0.16 mA M^{-1}	1.6×10^{-4} to 11.5×10^{-3}	55	94 over 20 days	Wen et al. [56]
PtE/PAA/MWCNTs/Cyst/AuNPs/GOx	2.527 mA M^{-1}	1.0×10^{-4} to 10.0×10^{-3}	6.7	92 over 30 days	Wu et al. [57]
GCE/MWCNTs-Gr-PDDA-AuNPs/GOx	29.72 mA M^{-1} cm^{-2}	3.0×10^{-4} to 2.1×10^{-3}	4.8	89 over 21 days	Yu et al. [58]
GCE/MWCNTs-PVA-GOx/AuNPs	16.6 mA M^{-1} cm^{-2}	5.0×10^{-4} to 8.0×10^{-3}	200	–	Zhang et al. [59]
GCE/bMWCNTs-HBPEI/AuNPs-B(OH)$_2$/GOx	3.26 mA M^{-1} 28.6 mA M^{-1} cm^{-2}	2.5×10^{-4} to 5.0×10^{-3}	0.8	86.1 over 14 days	This work

ACS, alumina coated silica; AgNPs, silver nanoparticles; AuNPs, gold nanoparticles; Chit, chitosan; Con A; concanavalin A; Cyst, cysteamine; GCE, glassy carbon electrode; Gr, graphene; IL, ionic liquid; ITO; indium tin oxide; MWCNTs, multiwalled carbon nanotubes; Nf, nafion; pDA, polydopamine; PAA, poly(allylamine); PDDA, poly(diallydimethylammonium); PE, paste electrode; PSS, poly(sodium 4-styrene-sulfonate); PtE, platinum electrode; PtNPs, platinum nanoparticles; PVA, polyvinyl alcohol; ZnONPs, zinc oxide nanoparticles.

absence and presence of 0.070 M glucose at 0.250 V. A characteristic S-shaped catalytic wave was obtained (Fig. SI2) due to the biocatalytic oxidation of glucose according to the well-known mechanism shown in the SI. The constant values used for the calculation, taken from the pioneering work of Bourdillon et al. under similar experimental conditions, were $k_2 = 780\ s^{-1}$, $k_3 = (6.2 \pm 0.5) \times 10^6\ M^{-1}\ s^{-1}$, and $k_{red} = 1.2 \times 10^4\ M^{-1}\ s^{-1}$ [44]. Under our experimental conditions, Γ_{GOx} was 2.2×10^{-11} mol cm^{-2} (assuming a two-electron transfer reaction), which is three times higher than the value of 7.6×10^{-12} mol cm^{-2} obtained for GCE/bMWCNTs-PEI/GOx. These results suggest that the bMWCNTs-PEI/AuNPs-B(OH)$_2$ hybrid material provides a large and effective surface-area for enzyme immobilization retaining its biocatalytic activity.

3.5. Analytical performance of the biosensor

Fig. 6A displays the amperometric recordings obtained at 0.700 V with the GCE/bMWCNTs-PEI/AuNPs-B(OH)$_2$/GOx biosensor for successive additions of 2.5×10^{-4} M glucose. A fast response was observed after the addition of glucose, 95% of the steady-state current being reached in 3 s. Fig. 6B shows the calibration plot obtained from the amperometric recordings ($n = 10$). A linear range ($r = 0.998$) between 2.50×10^{-4} M and 5.00×10^{-3} M was achieved with a sensitivity of (3.26 ± 0.03) mA M^{-1} (28.6 mA M^{-1} cm^{-2}). The detection limit was 0.8 μM (taken as $3.3\sigma/S$, where σ is the standard deviation of the blank signal and S, the sensitivity), and the quantification limit, 2.4 μM (taken as $10\sigma/S$).

The GCE/bMWCNTs-PEI/AuNPs-B(OH)$_2$/GOx revealed a high reproducibility, with a relative standard deviation value of 4.5% calculated from the slope values of the glucose calibration plots obtained with ten different biosensors. The reusability of the same biosensor surface was also good, yielding a relative standard deviation of 8.6% for ten successive calibrations. The long-term stability of the bioelectrode was also checked by storing at 4 °C under dry conditions and measuring the response to glucose once a day. The biosensor retained 90.2% and 86.1% of its original response after 9 and 14 days of storage, respectively. This behavior can be attributed to the strong attachment of the enzyme on the AuNPs-B(OH)$_2$ and also to the proper biocompatibility of the hybrid nanomaterial that offer a friendly environment for GOx immobilization.

The analytical performance of GCE/bMWCNTs-PEI/AuNPs-B(OH)$_2$/GOx was compared to that of other reported glucose biosensors involving hybrids of carbon nanotubes and nanoparticles (Table 1). The biosensor possesses an excellent detection limit which is the lowest of those summarized in Table 1 and comparable to that obtained with specific GOx immobilization with concavalin A lectin [48]. A good sensitivity, which is better than most of the values reported in Table 1, and a linear range which is comparable to most of those indicated in Table 1, have been obtained with the proposed biosensor. Although the biosensor constructed by immobilizing GOx on carbon nanotube-alumina coated silica-platinum nanoparticles composite film [52] showed a better sensitivity, it should be pointed out that its detection limit is one order of magnitude greater. Our biosensor exhibits additional advantages like the supramolecular mechanism for the biosensor construction without covalent methods and a good long-term stability due to the biocompatibility of the nanohybrid material for enzyme immobilization.

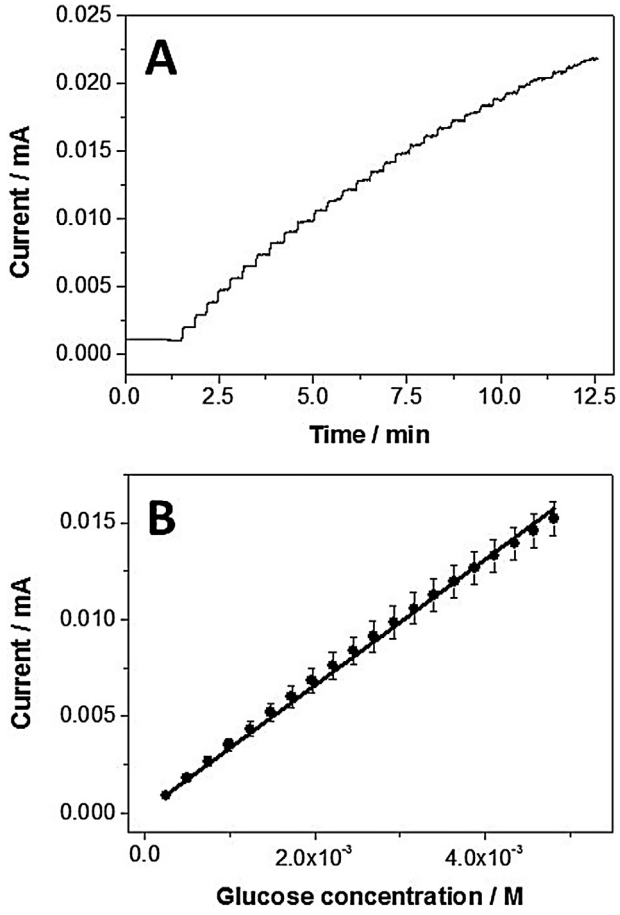

Fig. 6. (A) Amperometric recording obtained at 0.700 V for successive additions of 2.5×10^{-4} M glucose at GCE/bMWCNTs-PEI/AuNPs-B(OH)$_2$/GOx. (B) Calibration plot obtained from the amperometric recording shown in (A) (the calibration plot was obtained using ten different electrodes).

Table 2
Determination of glucose in real samples.

Sample	Glucose (g/100 mL)		RSD (%)	Recovery (%)
	Reported	Found		
Pepsl	3.9	4.0 ± 0.1	2.5	102 ± 3
Gatorade	2.4	2.4 ± 0.1	4.2	100 ± 5
Red Bull	3.6	3.6 ± 0.1	2.8	101 ± 3
Sample	Glucose (M)		RSD (%)	Recovery (%)
	Reported	Found		
Milk	3.9×10^{-2}	$(3.8 \pm 0.2) \times 10^{-2}$	4.0	98 ± 4

The kinetics parameters of the biosensor obtained from Eadie–Hofstee plots were $K_M^{app} = (8.1 \pm 0.5) \times 10^{-3}$ M and $I_{max} = (41 \pm 3)$ μA. This K_M^{app} value is smaller than those reported for the native GOx in solution (27 mM) [60], suggesting the high affinity of the enzyme towards glucose when it is immobilized on the nanohybrid material.

The GCE/bMWCNTs-PEI/AuNPs-B(OH)$_2$/GOx biosensor was used to determine the glucose content in commercial soft drinks (Pepsi®, Gatorade® and Redbull®) and baby milk samples ("Crecer 1" milk for babies from 0 to 6 months, Argentine dairy company "La Serenísima"). In order to minimize matrix effects, the determination of glucose was accomplished by using the standard additions method. Table 2 compares the concentration of glucose obtained with the biosensor with the values reported by the supplier. There is an excellent agreement between both values, demonstrating the analytical reliability of the proposed electrochemical device to quantify glucose in real samples. Considering additional practical applications, we also evaluated the interference of two easily oxidizable compounds, ascorbic (AA) and uric acid (UA). Since both compounds interfere in the determination of 5.0×10^{-4} M glucose (34% for 1.0×10^{-5} M AA and 23% for 5.0×10^{-5} M UA), we incorporated an outer layer (5.0 μL) of commercial Nafion diluted ten times with 0.050 M phosphate buffer pH 7.40 (0.50%, v/v) at GCE/bMWCNTs-PEI/AuNPs-B(OH)$_2$/GOx. Under those conditions, the interference decreased to 8.0 and 6.0% for AA and UA, respectively, expanding in this way the possibilities of analytical applications of the proposed biosensor.

4. Conclusions

This work reports a new bioanalytical platform based on the deposition at GCE of a hybrid material obtained from the association of AuNPs-B(OH)$_2$ and bMWCNTs and further incorporation of the model enzyme GOx. Even when there are hundreds of works dealing with electrochemical glucose biosensing, the strategy proposed here is really innovative since it associates the synergistic effect of the hybrid material for the oxidation of hydrogen peroxide with the selective immobilization of GOx through the boronic acid residues. The biosensor demonstrated to possess a very competitive analytical performance and a successfully application for the quantification of glucose in beverages and milk sample, with excellent correlation with the reported values.

The platform described here represents a very versatile alternative not only for the preparation of glucose biosensors, but also for other type of biosensors just by selecting a biomolecule able to be recognized by boronic acid, opening the way to the development of new biosensors.

Acknowledgements

The authors thank CONICET, ANPCyT, SECyT-UNC, MINCyT-Córdoba for the financial support. M.E. thanks CONICET for the postdoctoral fellowship.

Appendix A. Supplementary data

Supplementary data associated with this article can be found, in the online version, at http://dx.doi.org/10.1016/j.snb.2015.03.112

References

[1] C. Zhu, G. Yang, H. Li, D. Du, Y. Lin, Anal. Chem., http://dx.doi.org/10.1021/ac5039863
[2] A. Walcarius, S.D. Minteer, J. Wang, Y. Lin, A. Mercoci, J. Mater. Chem. B 1 (2013) 4878–4908.
[3] C.I.L. Justino, T.A.P. Rocha-Santos, S. Cardoso, A.C. Duarte, Trends Anal. Chem. 47 (2013) 27–36.
[4] C.I.L. Justino, T.A.P. Rocha-Santos, A.C. Duarte, Trends Anal. Chem. 45 (2013) 24–36.
[5] G. Doria, J. Conde, B. Veigas, L. Giestas, C. Almeida, M. AssunÇao, J. Rosa, P.V. Baptista, Sensors 12 (2012) 1657–1687.
[6] J.S. Beveridge, J.R. Stephens, M.E. Williams, Annu. Rev. Anal. Chem. 4 (2011) 251–273.
[7] J. Yuan, A.H.E. Müller, Polymers 51 (2010) 4015–4036.
[8] R. Villalonga, P. Díez, M. Eguílaz, P. Martínez, J.M. Pingarrón, ACS Appl. Mater. Interfaces 4 (2012) 4312–4319.
[9] S. Suresh, M. Gupta, G.A. Kumar, V.K. Rao, O. Kumar, P. Ghosal, Analyst 137 (2012) 4086–4092.
[10] M. Eguílaz, R. Villalonga, L. Agüí, P. Yáñez-Sedeño, J.M. Pingarrón, J. Electroanal. Chem. 1 (2011) 171–178.
[11] P. Nayak, B. Anbarasan, S. Ramaprabhu, J. Phys. Chem. C 117 (2013) 13202–13209.
[12] M. Eguílaz, R. Villalonga, P. Yáñez-Sedeño, J.M. Pingarrón, Anal. Chem. 83 (2011) 7807–7814.
[13] M.L. Yola, T. Eren, N. Atar, Biosens. Bioelectron. 60 (2014) 277–285.

[14] E.N. Primo, F.A. Gutierrez, G.L. Luque, P.R. Dalmasso, A. Gasnier, Y. Jalit, M. Moreno, M.V. Bracamonte, M. Eguílaz Rubio, M.L. Pedano, M.C. Rodríguez, N.F. Ferreyra, M.D. Rubianes, S. Bollo, G.A. Rivas, Anal. Chim. Acta 805 (2013) 19–35.
[15] D. Tuncel, Nanoscale 3 (2011) 3545–3554.
[16] P.C. Ma, N.A. Siddiqui, G. Marom, J.K. Kim, Composites: Part A 41 (2010) 1345–1367.
[17] W. Yang, Y. Wang, J. Li, X. Yang, Energy Environ. Sci. 3 (2010) 144–149.
[18] M.A. Correa-Duarte, L.M. Liz-Marzán, J. Mater. Chem. 16 (2006) 22–25.
[19] Y.Y. Huang, E.M. Terentjev, Polymer 4 (2012) 275–295.
[20] P.R. Dalmasso, M.L. Pedano, G.A. Rivas, Biosens. Bioelectron. 39 (2013) 76–81.
[21] Y. Jalit, M. Moreno, F.A. Gutierrez, A. Sanchez-Arribas, M. Chicharro, E. Bermejo, A. Zapardiel, C. Parrado, G.A. Rivas, M.C. Rodríguez, Electroanalysis 25 (2013) 1116–1121.
[22] J. Li, Z. Wang, P. Li, N. Zong, F. Li, Sens. Actuators B 161 (2012) 832–837.
[23] Y. Wang, S. Chalagalla, T. Li, X. Sun, W. Zhao, P.G. Wang, Z. Zeng, Biosens. Biolectron. 26 (2010) 996–1001.
[24] R. Wannapob, P. Kanatharana, W. Limbut, A. Numnuam, P. Asawatreratanakul, C. Thammakhet, P. Thavarungkul, Biosens. Bioelectron. 26 (2010) 357–364.
[25] K.M. Hsieh, K.C. Lan, W.L. Hu, M.K. Chen, L.S. Jang, M.H. Wang, Biosens. Bioelectron. 49 (2013) 450–456.
[26] D.M. Kim, Y.B. Shim, Anal. Chem. 85 (2013) 6536–6543.
[27] S.E. Diltemiz, A. Ersöz, D. Hür, R. Keçili, R. Say, Mater. Sci. Eng. C 33 (2013) 824–830.
[28] Z. Wang, Y. Tu, S. Liu, Talanta 77 (2008) 815–821.
[29] J.A. Ho, W.L. Hsu, W.C. Liao, J.K. Chiu, M.L. Chen, H.C. Chang, C.C. Li, Biosens. Bioelectron. 26 (2010) 1021–1027.
[30] M. Moreno-Guzmán, I. Ojeda, R. Villalonga, A. González-Cortés, P. Yáñez-Sedeño, J.M. Pingarrón, Biosens. Bioelectron. 35 (2012) 82–86.
[31] Y. Ben-Amram, M. Riskin, I. Willner, Analyst 135 (2010) 2952–2959.
[32] M. Frasconi, R. Tel-Vered, M. Riskin, I. Millner, Anal. Chem. 82 (2010) 2512–2519.
[33] Q. Wang, L. Yang, X. Yang, K. Wang, J. Liu, Analyst 138 (2013) 5146–5150.
[34] N. Xia, D. Deng, L. Zhang, B. Yuan, M. Jing, J. Du, L. Liu, Biosens. Bioelectron. 43 (2013) 155–159.
[35] M. Liu, L. Zhang, Y. Xu, P. Yang, H. Lu, Anal. Chim. Acta 788 (2013) 129–134.
[36] R. Villalonga, P. Díez, P. Yáñez-Sedeño, J.M. Pingarrón, Electrochim. Acta 56 (2011) 4672–4677.
[37] C. Amatore, N. Da Mota, C. Lemmer, C. Pebay, C. Sella, L. Thouin, Anal. Chem. 80 (2008) 9483–9490.
[38] R. Villalonga, P. Díez, S. Casado, M. Eguílaz, P. Yáñez-Sedeño, J.M. Pingarrón, Analyst 137 (2012) 342–348.
[39] J.A. Faniran, H.F. Shurvell, Can. J. Chem. 46 (1968) 2089–2095.
[40] M.D. Rubianes, G.A. Rivas, Electrochem. Commun. 9 (2007) 480–484.
[41] M. Eguílaz, N.F. Ferreyra, G.A. Rivas, Electroanalysis 26 (2014) 2434–2444.
[42] Q. Shao, P. Wu, X. Xu, H. Zhang, C. Cai, Phys. Chem. Chem. Phys. 14 (2012) 9076–9085.
[43] N.F. Ferreyra, L. Coche-Guerente, P. Labbé, Electrochim. Acta 49 (2004) 477–484.
[44] C. Bourdillon, C. Demaille, J. Moiroux, J-M. Saveant, J. Am. Chem. Soc. 115 (1993) 2–10.
[45] F. Hu, S. Chen, C. Wang, R. Yuan, Y. Chai, Y. Xiang, C. Wang, J. Mol. Catal. B 72 (2011) 298–304.
[46] F. Jia, C. Shan, F. Li, L. Niu, Biosens. Bioelectron. 24 (2008) 945–950.
[47] F. Li, Z. Wang, C. Shan, J. Song, D. Han, L. Niu, Biosens. Bioelectron. 24 (2009) 1765–1770.
[48] W. Li, R. Yuan, Y. Chai, H. Zhong, Y. Wang, Electrochim. Acta 56 (2011) 4203–4208.
[49] J. Manso, M.L. Mena, P. Yáñez-Sedeño, J. Pingarrón, J. Electroanal. Chem. 603 (2007) 1–7.
[50] R.B. Rakhi, K. Sethupathi, S. Ramaprabhu, J. Phys. Chem. B 113 (2009) 3190–3194.
[51] D. Ragupathy, A.I. Gopalan, K.P. Lee, Electrochem. Commun. 11 (2009) 397–401.
[52] M.C. Tsai, Y.C. Tsai, Sens. Actuators B 141 (2009) 592–598.
[53] H.J. Wang, C.M. Zhou, F. Peng, H. Yu, Int. J. Electrochem. Sci. 2 (2007) 508–516.
[54] Y. Wang, W. Wei, X. Liu, X. Zeng, Mater. Sci. Eng. C 29 (2009) 50–54.
[55] Y. Wang, L. Liu, M. Li, S. Xu, F. Gao, Biosens. Bioelectron. 30 (2011) 107–111.
[56] Z. Wen, S. Ci, J. Li, J. Phys. Chem. C 113 (2009) 13482–13487.
[57] B.Y. Wu, S.H. Hou, F. Yin, Z.X. Zhao, Y.Y. Wang, X.S. Wang, Q. Chen, Biosens. Bioelectron. 22 (2007) 2854–2860.
[58] Y. Yu, Z. Chen, S. He, B. Zhang, X. Li, M. Yao, Biosens. Bioelectron. 52 (2014) 147–152.
[59] H. Zhang, Z. Meng, Q. Wang, J. Zheng, Sens. Actuators B 158 (2011) 23–27.
[60] M.J. Rogers, K.G. Brandt, Biochemistry 10 (1971) 4624–4630.

Biographies

Marcos Eguílaz received his degree in Chemical sciences with a specialization in Environment from the Complutense University of Madrid (Madrid, España) in 2006 and his Ph.D. in Analytical chemistry in 2012 from the same university. He performed post-doctoral research in the group of Electroanalysis and Electrochemical (bio)sensors of the Complutense University of Madrid between 2012 and 2013. At present, he is a postdoctoral fellow of CONICET in the Biosensors Group at the Physical Chemistry Department, Faculty of Chemical Sciences, National University of Cordoba, Argentina. His postdoctoral research is focused on the design and characterization of bio-functional analytical platforms based on carbon nanotubes and graphene functionalized with polymers.

Reynaldo Villalonga was graduated at the University of Havana, Cuba with his Gold Diploma in 1993. During 1994 he worked on protein structures at the National Center for Genetic Engineering and Biotechnology and then joined the Laboratory of Bioinorganic Chemistry at the University of Havana. In 1996 he moved to the University of Matanzas, where he founded the Enzyme Technology Group and started working on neoglycoenzymes. He completed his Ph.D. degree in neoglycoenzyme synthesis in 2001 and was appointed as Full Professor and Founding Director of the Center for Enzyme Technology at the University of Matanzas in 2007. In 2010 he moved to the Complutense University of Madrid, Spain, where he held a Ramón y Cajal Research Professorship. He was a visiting Professor at the University of Naples "Federico Segundo", McGill University, Toyama Prefectural University, Firenze University, Vigo University and Joseph Fourier University. His research is focused on neoglycoenzymes, carbohydrate chemistry, drug delivery systems, biosensors and nanotechnology. He has been recognized with several honors and awards including seven prizes from the Cuban Academy of Sciences, the Development Cooperation Prize of Belgium (2001), the Third World Academy of Sciences Award for Young Chemist (2004), the National Award in Chemical Sciences (2006), the Prize of the Cuban Ministry of Science (2007), the Prize of Ministry of Higher Education (2004, 2007), the Japanese Society for the Promotion of Science Fellowship (2004, 2008) and the Carolina Foundation Fellowship (2007). Since 2001 he has promoted and organized the Latin American Network for Enzyme Technology "RELATENZ".

J.M. Pingarrón obtained his Ph.D. (1981) from Complutense University of Madrid. Between 1982 and 1983, he did postdoctoral training at the École Nationale Supérieure de Chimie de Paris. Since 1994, he is a full Professor of Analytical Chemistry at the Complutense University of Madrid. José M. Pingarrón headed the Department of Analytical Chemistry at the Faculty of Chemistry between 1998 and 2006 and he was the President of the Spanish Society of Analytical Chemistry between 1998 and 2001. Professor Pingarrón is the recipient of the Faculty of Chemistry Medal, the Complutense University of Madrid Medal and the research award on Analytical Chemistry of the Spanish Royal Society of Chemistry. His research interests focus on analytical electrochemistry, nanostructured electrochemical interfaces and electrochemical and piezoelectric sensors and biosensors. He has over 270 publications including peer-reviewed papers, book chapters and text books. He is currently Vice-President of the Spanish Royal Society of Chemistry and is its representative in the Division of Analytical Chemistry of the European Association for Chemical and Molecular Sciences. Professor Pingarrón is Associate Editor of Electroanalysis journal and belongs to the Editorial Advisory Boards of the Journal of Electroanalytical Chemistry, Talanta, Analyst, Chemical Sensors and ChemElectroChem and Member of the Analytical Chemistry Division Committee of IUPAC. Moreover, Professor Pingarrón is co-founder of the "spin-off" company Inbea Biosensores S.L.

Nancy F. Ferreyra obtained her Ph.D. in Chemistry in 2002 from the National University of Córdoba (Argentina). She performed her postdoctoral training at Université Joseph Fourier (Grenoble, France). In 2004 she joined the team headed by Prof. Rivas at Physical Chemistry Department, Faculty of Chemical Sciences, National University of Córdoba. She is currently Full Professor and Independent Researcher at National Research Council (CONICET, Argentina). Her research interests are focused on the development of supramolecular structures to study bio-recognition reactions involving glycoproteins.

Gustavo A. Rivas obtained his Ph.D. in chemistry (1991) from Cordoba National University (Cordoba, Argentina). He did the postdoctoral training at University of Valence, Valence (Spain) in 1994 and 1995 and at New Mexico State University, Las Cruces (USA) between 1995 and 1996. At present, he is Full Professor at Cordoba National University and Superior Researcher at Argentine Research Council (CONICET). Dr. Rivas was the Head of the Department of Physical Chemistry at the Faculty of Chemical Sciences between 2008 and 2010. He was President of the Argentinean Society of Analytical Chemists between 2005 and 2007. Professor Rivas is the recipient of the Ranwell Caputto Award from National Academy of Sciences of Argentina (2001), Rafael Labriola Award from Argentinean Society of Chemistry (2004), and Konex Award in Nanotechnology (2013). His research interests focus on the design and characterization of electrochemical (bio)sensors based on nanostructured materials, the development of new bioanalytical platforms for biosensing in batch and flow systems, the study of DNA damage, and the design of new strategies for nanomaterials and polymers modification.